ELSEVIER

Cortex

Special Issue 'From Bodies to Spaces': a neurocognitive/neuropsychological...':
Research Report

Shared body representation constraints in human and non-human primates behavior

A. Errante [a], A. Rossi Sebastiano [b], N. Castellani [b,c], S. Rozzi [a], L. Fogassi [a] and F. Garbarini [b,d],*

[a] Department of Medicine and Surgery, University of Parma, Parma, Italy
[b] MANIBUS Lab, Psychology Department, University of Turin, Turin, Italy
[c] MoMiLab, IMT School for Advanced Studies, Lucca, Italy
[d] Neuroscience Institute of Turin (NIT), Turin, Italy

ARTICLE INFO

ABSTRACT

Previous studies indicated that the sense of body ownership (i.e., the feeling that our body parts belong to us; SBO) can be experimentally modulated in humans. Here, we focused on SBO from an across-species perspective, by investigating whether similar bottom-up and top-down constraints that consent to build SBO in humans also operate to build it in monkeys. To this aim, one monkey and a cohort of humans ($N = 20$) performed a paradigm combining the well-known rubber hand illusion (RHI), able to induce a fake hand embodiment, and a hand-identification reaching task, borrowed from the clinical evaluation of patients with SBO disorders. This task consisted of reaching one's own hand with the other, while presenting a fake hand in different conditions controlling for bottom-up (synchronicity of the visuo-tactile stimulation) and top-down (congruency of the fake hand position relative to the monkey's body) SBO constraints. Spatiotemporal kinematic features of such self-directed movements were measured. Our results show that, when the monkey aimed at the own hand, the trajectory of self-directed movements was attracted by the position of the hand believed to be one's own (i.e., the fake hand), as in humans. Interestingly, such an effect was present only when both bottom-up and top-down constraints were met. Moreover, in the monkey, besides displacement of movement trajectory, also other kinematic parameters (velocity peak, deceleration phase) showed sensitivity to the embodiment effect. Overall, if replicated in a larger sample of monkeys, these results should support the view that human and non-human primates share similar body representation constraints and that they are able to modulate the motor behavior in both species.

* *Corresponding author.* Psychology Department, University of Turin, Manibus Lab Coordinator, Via Verdi, 10 −10124, Torino, Italy.
E-mail address: francesca.garbarini@unito.it (F. Garbarini).

1.   Introduction

A challenge for neuroscience is to understand our *sense of body ownership* (SBO); i.e., the feeling that body parts belong to us (Gallagher, 2000). A vast literature has largely explored this topic in humans, by revealing neural mechanisms that sustain this function (Castro et al., 2023), as well as behavioral rules and constraints that allow its emergence (Blanke, Slater, & Serino, 2015). Although the SBO is likely shared among different species, less attention has been paid on it outside the human context. In the present study, we focused on non-human primates, and we asked whether similar constraints, that consent to build SBO in humans, also operate to build it in monkeys. To this aim, we capitalized on consolidated procedures in humans, able to alter the SBO in healthy participants, such as the rubber hand illusion (RHI) (Botvinick & Cohen, 1998), and to evaluate its selective dysfunction in pathological contexts, such as pathological embodiment (Candini et al., 2022; Errante et al., 2022; Garbarini et al., 2013, 2014; Rossi Sebastiano et al., 2022; see below). Thus, we combined these two approaches in a novel paradigm suitable for investigating the monkey's behavior. Starting from the RHI, we took advantage of this multisensory illusion, in which the synchronous stroking of the participant's real hand (occluded from view) as well as that of a clearly visible human-like fake hand, congruently positioned with respect to the participant's posture and perspective, leads experimental subjects to feel as if the fake hand were their own (the so-called *embodiment*). Several studies exploiting this procedure in healthy participants have revealed that some rules must be respected in order to observe the embodiment phenomenon, thus shedding light on the constraints that allow building a normal SBO. Indeed, illusory embodiment is ruled not only by bottom-up factors (i.e., the synchronicity of the strokes applied to the real and the fake hand) but also by top-down constraints (i.e., the congruency of the fake hand's position relative to the participant's body) (Blanke et al., 2015). In agreement with human studies, previous studies on rodent models already exploited the RHI to suggest that mice may experience body ownership of their tail (Buckmaster, Rathmann-Bloch, de Lecea, Schatzberg, & Lyons, 2020; Wada, Takano, Ora, Ide, & Kansaku, 2016, 2019). In non-human primates, pioneering studies investigate neurophysiological alterations induced by the RHI. For instance, it has been shown that, during the synchronous stimulation of the monkey's real and fake arms, bimodal, tactile and visual neurons in the ventral premotor cortex and posterior parietal area 5 not only respond to the felt position of the real arm when it is covered from view, but also to the seen position of a fake arm (Graziano, 1999; Graziano, Cooke, & Taylor, 2000). Furthermore, more recent evidence demonstrated that following a period of illusion induction, the monkey's neurons in S1 and M1 start responding also when tactile stimuli are applied to the fake hand alone (Shokur et al., 2013), further demonstrating that the monkey's neural circuitry is deeply altered during multisensory illusions. However, whether these neural events are also accompanied by a modulation of the monkey's behavior is still unknown. In Graziano's words *"We did not know if the false arm "fooled" the monkey, but we could study its influence on the behavior of neurons"* (Graziano, 1999, 2000).

In the present study, we combined a modified version of the RHI to induce body ownership alterations in a Rhesus monkey (and in a group of human controls) with an *ad hoc* procedure. This procedure derives from a clinical evaluation that we previously designed in a pathological context and now modified to investigate the monkey's behavior following the illusion induction. In particular, we focused on a mono-thematic delusion of body ownership after brain-damage that we named *pathological embodiment,* since patients show a systematic misattribution of someone else's hand to their own body [e.g., (Candini et al., 2022; Errante et al., 2022; Garbarini et al., 2013, 2014; Rossi Sebastiano, Poles, et al., 2022)]. Importantly, in these patients, pathological embodiment occurs only when the constraints of an aprioristic body representation, as those demonstrated using the RHI, are respected. Indeed, the alien (i.e., the examiner's) hand is embodied only when it is placed in an egocentric body-congruent position, aligned to the patient's shoulder. In this condition, when patients are asked to identify the own affected hand, by reaching it with the unaffected one, they systematically reach for the alien hand, identifying it as their own. By contrast, when the alien hand is misaligned to the patient's shoulder (body-incongruent position), the pathological embodiment does not occur [for a review see (Garbarini, Fossataro, Pia, & Berti, 2020)].

In our preliminary investigation, we collected data from one monkey and a cohort of 20 humans. Based on the above described hand-identification reaching task, we designed an *ad-hoc* paradigm in which we alternated 13−15 sec of RHI, able to induce embodiment over a fake hand, and reaching movements, in which the monkey was trained (and human controls were instructed) to reach for the hand exposed to the illusion (i.e., the left one) with the non-deluded hand (i.e., the right one). Thereby, we created a non-verbal task (i.e., hand-identification reaching task) to test the embodiment over the fake hand by employing fully implicit measures (i.e., kinematic parameters). To investigate whether, in monkey as in humans, illusory embodiment is ruled by both bottom-up factors and top-down constraints, we manipulated the synchronicity of visuo-tactile stimulation and the congruency of the fake hand position relative to the monkey's body, respectively. Thus, in our (2 × 2) factorial design, visuo-tactile stimulations could be either synchronous (known to induce the embodiment) or asynchronous (known to not); the fake hand position could be either aligned (*internal position*, known to induce the embodiment) or misaligned to the shoulder (*external position*, known to not). Spatial and temporal shifts of kinematic parameters toward the fake hand, depending on the experimental conditions, should allow us both to address the occurrence of the embodiment phenomenon in the monkey's behavior and to test whether it is ruled by the same constraints regulating the body representation in humans.

2. Methods

2.1. Participants

2.1.1. Human controls
Twenty-eight human volunteers (16 females; mean age ± standard deviation: 25.81 ± 7.12 years; range 20—59 years) participated in the study. All human controls had normal or corrected-to-normal vision. Only individuals with no history of neurological, orthopedic or rheumatological diseases, and no drug or alcohol abuse were recruited. All human controls were right-handed according to the Edinburgh Handedness Scale (Oldfield, 1971). Eight controls were subsequently excluded from data analysis due to technical problems during data acquisition. Overall, 20 human controls were included in the successive analyses (12 females; mean age ± standard deviation: 26.42 ± 8.25 years; range 20—59 years). Informed consent was obtained in accordance with ethical standards set out by the Declaration of Helsinki (1964). The study was approved by the ethical committee of the University of Turin (Prot. 133, 278 7/03/2019).

2.1.2. Monkey
The experiment was carried out on a male Rhesus monkey (Macaca Mulatta) weighing about 10 kg. All methods were performed in accordance with relevant guidelines and regulations. Animal handling, as well the behavioral procedures, complied with the European (directives 86/609/EEC, 2003/65/CE, and 2010/63/EU) and Italian (D.L. 116/92 and 26/2014) laws in force on the humane care and use of laboratory animals. All procedures were approved by the Veterinarian Animal Care and Use Committee of the University of Parma and authorized by the Italian Ministry of Health.

2.2. Apparatus and behavioral paradigm

2.2.1. Human controls
The participants sat on a chair in front of a table, on which a wooden apparatus (32 × 100 × 65 cm), similar to that used in the monkey experiment (see below), but adapted for human subjects, was placed. The apparatus had a removable horizontal opaque panel that could be placed on its upper part (occluding the participant left forelimb from vision). In the starting position, human controls placed their hands inside the apparatus with the palm down. In this rest position they were required to hold their right and left index fingers on marked points. The starting point of the right hand was placed on the right side at 20 cm from the body midline. In both baseline and experimental conditions, a rubber left hand (fake hand), matching the participant's biological gender, was introduced. Hence, on the left side of the apparatus, the two left hands (i.e., the participant's left hand and the fake one) could be placed in two possible configurations: in the internal position, the fake hand was centered on the shoulder's axis (at about 20 cm from the body midline), being internally positioned between the participant's trunk and her left hand that was externally misaligned towards the left (at about 40 cm from the body midline); in the external position, the fake hand was externally misaligned to the shoulder towards the left (at about 40 cm from the body midline), while the participant's left hand was centered on the shoulder's axis (at about 20 cm from the body midline). On the horizontal plane, in front of each left hand, a red LED was positioned.

2.2.2. Monkey
The monkey faced a horizontal table consisting of a box, located at the belly height (dimensions 50 × 60 × 50 cm). The lower part of the box consisted of a horizontal plane (42 × 50 × 1.5 cm) on which three metal cylinders (starting point) were positioned, at about 20 cm from the monkey body. The first was aligned with the right shoulder of the monkey, while the other two were placed on the left, one in a medial position (internal cylinder), aligned with the monkey left shoulder, and the other in a lateral position (external cylinder), at about 5 cm from the previous one. The upper part of the box contained a transparent plexiglass frame (39 × 49 × 2 cm), at the shoulder level, tilted of about 8° in the antero—posterior axis, with the lowest part towards the monkey neck. This frame allowed to insert, depending on the condition, one opaque panel (39 × 10 × 1 cm), that could obscure either the internal position or the external one, making invisible the left hand of the monkey (see below, experimental paradigm).

In both baseline and experimental conditions, a fake left arm, similar to the monkey one (see Suppl. Fig. 1 for a representative image of the used fake arm), was introduced. The fake arm was made of fiberglass and covered with synthetic leather produced by a taxidermic procedure. As in the human experiment, the two left hands (i.e., the monkey's and the fake one) could be placed in two possible configurations: in the *external position*, the monkey's left hand held the internal cylinder while the fake held the external cylinder; in the *internal position*, the monkey's left hand held the external cylinder, while the fake hand held the internal cylinder. On the horizontal plane, in front of each left cylinder, a red LED was positioned.

2.3. Monkey training

At the beginning of the study, the monkey was habituated to the interaction with the experimenters in its home cage, by receiving food and being touched. Then, it was trained to leave the cage, to seat in a primate chair, and familiarize with the experimental setup. After this preliminary phase (lasting about 3 months), the monkey was trained to perform the hand identification reaching task. First, the monkey was trained to hold both hands on the starting points. Then, it was habituated to be touched by the experimenter on the left forearm without moving and, later on, to respond to the touch by reaching the stimulated body part with the right hand. Subsequently, the conditioning stimulus (touch) was substituted with the visual cue (LED). Finally, the monkey fake forelimb was introduced at the left-hand position not occupied by the monkey's own hand and the monkey was trained to fixate the fake hand, while an experimenter gently stroked with a brush both the monkey forelimb (from forearm to hand) and the fake one for about 2 min. This type of procedure was similar to the rubber hand illusion (RHI) procedure used in previous studies on humans (Botvinick & Cohen, 1998) and monkeys (Graziano

et al., 2000). Each phase of habituation and training was achieved by using a positive reinforcement technique. Reinforcement consisted in palatable food and liquids.

2.4. Rubber hand illusion procedure

Participants (monkey or human controls) placed their hands in the apparatus on the starting points, i.e., with the right hand on the corresponding marked point, and the left hand either in the internal or in the external position. The fake hand was placed in the internal/external position (not occupied by the real hand) and the opaque panel was introduced, preventing the participant from seeing her/his left hand, but allowing the view of the fake hand. In the human experiment, a white cloth covered the shoulders and the proximal parts of the left real and dummy hand, so that the participant could not appreciate the discontinuity between the rubber hand and the body. In the monkey experiment, the opaque panel was enough to prevent the view of such discontinuity. Then, the experimenter stroked the participant's left hand and the fake hand either synchronously or asynchronously for 2 min. In the synchronous (illusion) conditions, the stroking on the two hands was applied with the same timing. Conversely, in the asynchronous (control) conditions, the strokes on the real and fake hands were applied in anti-phase. This 2 min of stimulation was performed to allow the illusion to emerge (at least in the synchronous condition) and was immediately followed by the experimental procedure in which we alternated short blocks of stimulation with the hand-identification reaching task (see below).

2.5. Hand-identification reaching task

In the hand-identification reaching task (Fig. 1), human controls were instructed, and the monkey was trained, to reach and touch their left hand with their right one, starting from the right starting point. The enlightenment of the red LED was employed as a go signal for the movement. If the participant or the monkey performed additional movements of the arm at any time during the initial holding period, the trial was aborted. Participants were not allowed to make any correction once the pointing hand had reached the target hand. Note that, before each reaching movement, 10−12 sec of RHI stimulation was applied. This combined procedure allowed the illusion to be maintained throughout the experiment [see e.g., (della Gatta et al., 2016; Rossi Sebastiano, Bruno, et al., 2022; Rossi Sebastiano et al., 2022; Bruno et al., 2022) for similar procedures]. The task was repeated in four different
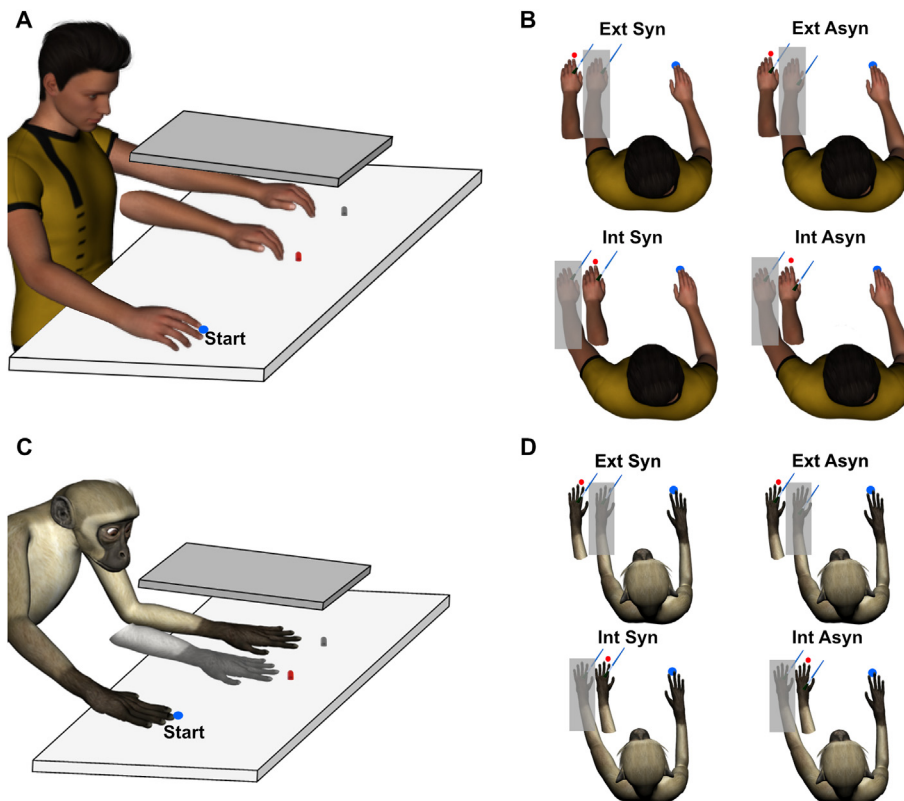

Fig. 1 − Illustration of the experimental paradigm carried out on human controls and the monkey. Before each trial, the subject remained in a rest state, with the hands on the starting points. In (A) and (C), an example of the internal position is depicted: the fake hand was placed in the internal position, aligned with the subject's left shoulder, while the real left hand was hidden from the view of the subject, by means of an opaque panel. (B, D) The paradigm consisted of four experimental conditions (see Methods). In all conditions, the fake hand was visible, while the real left hand was always hidden from the subject view. In each condition, after 10−12 s of visuo-tactile RHI stimulation, a red LED was switched on, prompting the subject to perform the reaching movement with the right hand towards the left hand.

experimental conditions: a) "external synchronous", the fake hand laid in the *external position* configuration and the *synchronous RHI stimulation* was applied; b) "external asynchronous", the fake hand laid in the *external position* configuration and the *asynchronous RHI stimulation* was applied; c) "internal synchronous", the fake hand laid in the *internal position* configuration and the *synchronous RHI stimulation* was applied; d) "internal asynchronous", the fake hand laid in the *internal position* configuration and the *asynchronous RHI stimulation* was applied (Fig. 1). Moreover, at the beginning of each session, we also collected two sets of trials in which the fake hand was presented but no RHI stimulation was applied, to characterize the kinematic profile of reaching movements in the internal and the external positions (i.e., "internal baseline", "external baseline" conditions).

In the human experiment, 180 trials (30 trials x 6 conditions) were collected, thus a total of 5040 trials (180 trials x 28 participants). The final analysis was carried out on 3600 trials (180 trials x 20 participants). In the monkey experiment, the entire dataset included a total of 600 trials: 100 correct trials for 6 conditions (4 main conditions, +2 baseline conditions), recorded in 5 days (20 trials per condition in each day). One hundred and twenty trials were subsequently excluded from the analysis due to technical problems or monkey errors. Note that these excluded trials were equally distributed between conditions (20 trials per conditions). Thus, the final dataset acquired in the monkey included a total of 480 trials.

In both human controls and in the monkey experiments, all the baselines and the experimental conditions were performed in separate blocks. In the human experiment, the order of the baseline conditions, always performed at the beginning of the session, was counterbalanced between participants, while the order of the following experimental conditions was randomized between participants. In between different conditions, a 5-min pause was required, in order to change the setting and also to cancel the effects of the illusion, preventing possible interactions with successive trials. In the monkey experiment, the order of the baseline conditions, always performed at the beginning of the session, was counterbalanced across sessions. The order of the following experimental conditions was counterbalanced between sessions: in half of the sessions the internal conditions were presented first, in the other half viceversa, alternating synchronous and asynchronous stimulation blocks. Similar to human controls experiment, also in the monkey experiment a 5-min pause was required between conditions, in order to change the setting and also to cancel the effects of the illusion.

2.6. Kinematic data acquisition and analysis

All performed reaching movements were video recorded and analyzed using 2D kinematic analysis. Data were acquired by means of a digital HD camera (© GoPro, Inc., USA), with a 240 frame/s rate and resolution of 1280 × 720p. The experiment consisted of 30 repetitions in human participants and 100 repetitions of the same action for each condition in the monkey. Note that, in the human controls sample, data from 8 subjects were discarded due to technical problems during kinematic data tracking. Thus, the final sample included 20 human controls.

Software Tracker (© Tracker v5.1.2, 2019 Douglas Brown) was used to measure the movement trajectory and velocity, by marking specific points placed on the subject hand. In the experiment on human controls the markers consisted of colored spheres (ø .5 cm) placed on the tip of the participant's right index finger. In the monkey experiment, a light blue colored marker was painted centered on the knuckle of the right little finger. The size of this latter marker was about 3 cm of diameter, thus larger with respect to that used for human controls, due the difficulty of automatically tracking a marker moving at high velocity (velocity peak about 360 cm/sec in the monkey versus 130 cm/sec in human controls). Using this arrangement, it was possible to calculate trajectory on x and y axes, and maximum peak velocity. The point of origin of the X/Y axes was set as the starting position of the subject's hand. To trace the markers, the auto-tracker function implemented in Tracker software was used. This procedure compares the image of the marker in each frame with its template image. More specifically, we created a point of mass in the center of the marker, using as tracking parameters an evolution rate of 20% and an auto-mark value of 4 (range 1—10). This setting reduces the probability of drifts in the template and false matches. Using these parameters, it was possible to trace marker position in the space every 4 msec until the end of the action. A line of 15 cm drawn on the side of the apparatus was used as a reference measure for software calibration. The calibration was computed by scaling the real distance measured in cm to the image distance expressed in pixels. Trajectory and velocity were calculated by using the co-ordinates of the point of mass on the x and y axis. Velocity index was calculated using a finite difference algorithm:

$$v = (x \cdot [i+1] - x \cdot [i-1]) / (2*dt)$$

where i refers to the step number and dt is the time between two consecutive steps expressed in ms. The velocity module accounts both for the x and y components, by calculating the combination of the two vector values, expressed in cm/sec. In order to account for the noise in the recorded data, values were averaged and smoothed by using a gaussian-weighted moving average filter included in Matlab R2020a (The Mathworks, Inc., Natick, MA, USA). In order to account for differences between trials having slightly different durations, we normalized each trial duration using the percentage of the total time and calculated and plotted mean velocity and trajectory data over movement time percentage.

2.7. Statistical analysis of kinematic data

2.7.1. Preliminary analyses on baselines
Three kinematic parameters were analyzed: the displacement of movement endpoint (calculated as the displacement on the x-axis of the final position in each condition), peak velocity (calculated as the maximal velocity reached in each condition's movement), and percentage of deceleration phase (computed as the percentage of deceleration phase observed in each movement of each condition). We chose to investigate

the displacement of movement endpoint on the *x*-axis towards the fake hand, because it reflects the measure most similar to that used for the evaluation of patients with "pathological embodiment" (E+), who, when asked to reach for their own affected hand with the unaffected one, systematically shift the movement endpoint along the *x*-axis, i.e., on the embodied hand.

As preliminary analyses, the values of each parameter were compared between the internal and external positions separately in the monkey and the human controls. To this aim, on each parameter, we performed two-tailed matched pairs *t*-tests between internal and external baselines.

2.7.2. Main analyses on experimental conditions

Since significant differences were found in the baselines analyses, revealing specific kinematic profiles for the two types of movements (i.e., internal versus external target hand position) (see Results section), before performing the main analyses on each kinematic parameter, we normalized the values of the experimental conditions on the corresponding baseline (i.e., using the internal baseline to normalize internal synchronous and asynchronous conditions and using the external baseline to normalize external synchronous and asynchronous conditions). First, the displacement of movement endpoint was calculated as the displacement on the *x*-axis of the final position in each condition relative to the endpoint position in the corresponding baseline. Note that positive and negative values were normalized so that, both in the case of the internal and the external positions, positive and negative values indicate a displacement towards or away from the fake hand, respectively. Second, the peak velocity was calculated as the difference between maximal velocity reached in each condition and that reached in the corresponding baseline. Third, the percentage of deceleration phase was computed as difference between the percentage of deceleration phase observed in each condition's movement and that observed in the corresponding baseline.

The resulting data of each parameter were analyzed using two different repeated-measures (rm)ANOVAs, one for the monkey dataset and the other for the human dataset. In the context of single animal studies rmANOVA is commonly used to take into account the correlation between measurements on the same case (Fang et al., 2019; Roy, Paulignan, Farnè, Jouffrais, & Boussaoud, 2000, 2002). Each dataset was entered as a dependent variable in a 2×2 repeated-measures ANOVA, with *Position* (external, internal) and *Stimulation* (synchronous, asynchronous) as repeated measures. Post-hoc comparisons were carried out by means of Newman–Keuls' test.

2.8. Explicit measures of RHI in human participants

In order to measure the effectiveness of the RHI procedures in the human experiment, explicit measures were additionally collected and analyzed. At the end of each block, participants were asked to rate their agreement with the items of the Embodiment questionnaire. Such questionnaire consisted of 3 "real" items, testing the feeling of embodiment, and 3 "control" items, controlling for response bias (Table 1) (Longo, Schüür, Kammers, Tsakiris, & Haggard, 2008).

Table 1 – Embodiment questionnaire.

1. It seemed as if I were sensing the touch in the location where I saw the rubber hand touched
2. It seemed as if the touch I felt was caused by the paintbrush touching the rubber hand
3. I felt as if the rubber hand was my hand
4. I felt as if my real hand was becoming a fake hand
5. I felt as if I had more than a left hand
6. I felt as if the rubber hand was shifting towards my left hand

Participants were asked to rate their agreement with the statements by assigning a score to each item, using a 7 points Likert Scale (−3 = "strongly disagree"; +3 = "strongly agree") (Longo et al., 2008). Note that the first three statements represent "real" items investigating the illusory feeling of ownership towards the fake hand, whereas the last three are "control" items, to control for response bias. Items were presented in a random order.

To compare the subjective feeling of embodiment toward the fake hand across conditions, an Embodiment index was computed as the delta between the mean ratings attributed to the real and the control items of the Embodiment questionnaire (embodiment index = real − control). Hence, high values of the embodiment index indicate strong feeling of embodiment. Values of the embodiment index were entered as a dependent variable in a 2×2 repeated-measures ANOVA, with *Position* (external, internal) and *Stimulation* (synchronous, asynchronous) as within-subject factors.

Post-hoc comparisons were carried out by means of Newman–Keuls' test. Before running parametric tests, normality of the residuals was checked by means of the Shapiro Wilk test (*p* always > .05). Statistical analyses were performed using Statistica Software (StatSoft, release 8).

3. Results

### 3.1. Kinematic study in human controls and monkey

3.1.1. Preliminary analyses on baselines

To characterize the kinematic profile of the movements performed in each position regardless of the RHI effect, at the beginning of each session, both human controls and the monkey performed the hand-identification reaching task without receiving the RHI visuo-tactile stimulation (i.e., "internal baseline" and "external baseline" conditions). Preliminary analyses of these baseline conditions suggest that movements performed in the internal and external positions are characterized by specific kinematic profiles, related to the different length of the movement trajectory between the two positions. Importantly, this specificity is present in both human controls and in the monkey, thus confirming that the movements executed by the two species during the task are comparable.
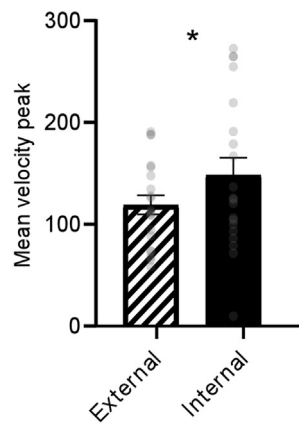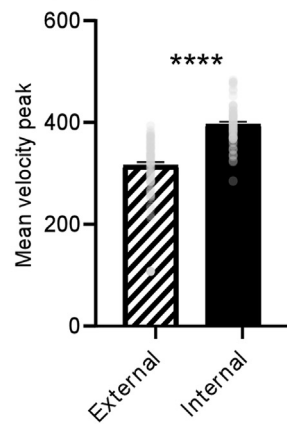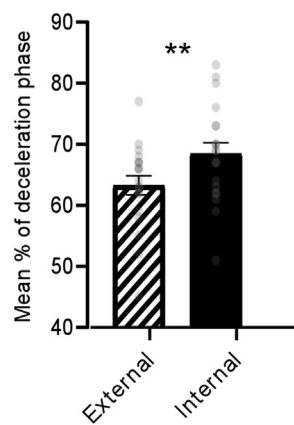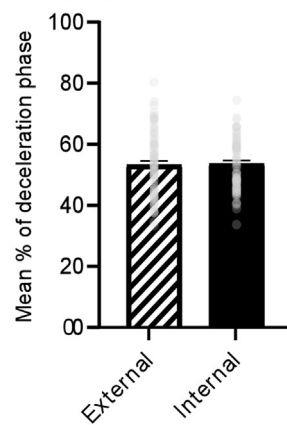
As regards the movement endpoint comparison between internal and external baselines, the matched pairs *t*-tests reveal, for both human controls [$t_{(1,19)} = 7.71$; $p = .0000003$] and the monkey [$t_{(1,79)} = 23.48$, $p = .00000001$], significantly greater values in the internal as compared to the external position

ANALYSES ON BASELINES

Human controls

A   **Movement endpoint**
$t_{(1,19)}=7.71$; $p< .0001$
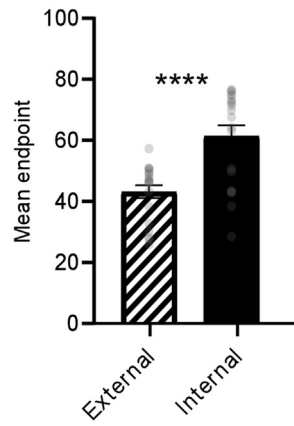
Monkey

B   **Movement endpoint**
$t_{(1,79)}=23.48$; $p< .0001$
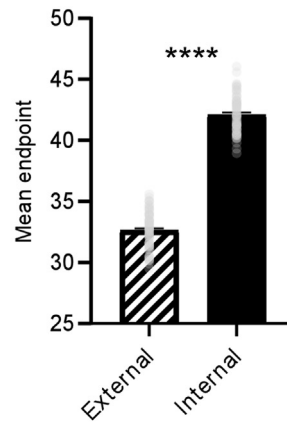
C   **Velocity peak**
$t_{(1,19)}=2.51$; $p= .02$

D   **Velocity peak**
$t_{(1,79)}=8.05$; $p< .0001$

E   **Deceleration phase**
$t_{(1,19)}=3.17$; $p= .005$

F   **Deceleration phase**
$t_{(1,79)}= .67$; $p= .51$

(Fig. 2A and B). This result is in line with the greater distance between the movement starting point and the *own* hand position in the internal (i.e., in which the fake hand is internally while the own one is externally displaced relative to the subject's shoulder) as compared to the external position (i.e., in which the own hand is internally while the fake one is externally displaced relative to the subject's shoulder).

As regards the velocity peak comparison between internal and external baselines, the matched pairs *t*-tests reveal, for both human controls [$t_{(1,19)} = 2.51$; $p = .02$] and the monkey [$t_{(1,79)} = 8.05$, $p = .000001$], significantly greater values in the internal as compared to the external position (Fig. 2C and D). This is in agreement with kinematic laws of biological movement showing that longer movements reach faster velocity (Castiello & Dadda, 2019; Castiello, Bennett, & Stelmach, 1993; Fogassi, Gallese, Gentilucci, Chieffi, & Rizzolatti, 1991, 2001; Jakobson & Goodale, 1991; Jeannerod, 1984; Messier & Kalaska, 1999; Sartori, Camperio-Ciani, Bulgheroni, & Castiello, 2013).

As regards the percentage of deceleration phase, by comparing internal and external baselines, the results show, only for humans [$t_{(1,19)} = 3.17$; $p = .005$], significantly greater values in the internal as compared to the external position (Fig. 2E). This finding is in agreement with kinematic laws of biological movement showing that longer movements require more on-line control during execution, thus resulting in a greater deceleration phase as compared to the acceleration phase (Castiello & Dadda, 2019). This difference was not significant in the monkey (Fig. 2F). A possible interpretation of this latter finding is that, in the monkey, baseline movements tend to be more ballistic, leading to less deceleration both in the internal and external conditions. This explains why, unlike in humans, the increase in speed observed in the external condition does not result in an increase in deceleration.

Due to the specific kinematic profile observed in preliminary analyses of baseline conditions, in the main analyses, we normalized each experimental condition on the corresponding baseline (see details in Methods). Thereby, we were able to test the modulation induced by both bottom-up (i.e., synchronicity of tactile stimulation) and top-down (i.e., congruency of the fake hand position with the body posture) constraints, regardless of the specific kinematic features characterizing the two different positions.

3.1.2. *Main analyses: displacement of movement endpoint results*

Mean movement trajectory for each of the four experimental conditions and the corresponding baselines is shown in Fig. 3A (human controls) and 3B (monkey). The displacement of movement endpoints is shown in Fig. 3C (human controls) and Fig. 3D (monkey). This parameter is a measure of the movement endpoint shift relative to the fake hand position, with values around zero indicating no modulation exerted by the rubber hand position, while positive and negative values

indicate a movement displacement towards or away from the fake hand respectively.

As expected, in human controls, the ANOVA shows a significant *Position by Stimulation* interaction [$F_{(1,19)} = 4.53$, $p = .047$], suggesting that, when both bottom-up and top-down constraints are respected (i.e., in the internal synchronous condition), the movement endpoint is significantly more shifted toward the fake arm as compared to all the other conditions (internal synchronous versus internal asynchronous: $p = .027$; internal synchronous versus external synchronous: $p = .014$; internal synchronous versus external asynchronous: $p = .028$) (Fig. 3C). This means that our protocol is effective in replicating classical RHI effects in humans. Crucially, the monkey's behavior fully parallels the results observed in humans. Indeed, the ANOVA shows again a significant *Position by Stimulation* interaction [$F_{(1,79)} = 8.86$, $p = .004$], with a greater movement displacement toward the fake hand during the internal synchronous condition as compared to all the other conditions (internal synchronous versus internal asynchronous: $p = .012$; internal synchronous versus external synchronous: $p = .0003$; internal synchronous versus external asynchronous: $p = .019$) (Fig. 3D). An opposite movement displacement away from the fake hand, although not significant ($p = .11$), was also present following Synchronous versus Asynchronous stimulation, when the fake arm was placed in the external body-incongruent position.

To sum up, this analysis reveals as an important new finding, that the monkey's behavior is affected by the illusory experience and that this happens only when the same bottom-up and top-down constraints operating in humans are respected.

3.1.3. *Main analyses: velocity peak and deceleration phase results*

Velocity profiles of human controls and the monkey are shown in Fig. 4A–B and C-D, respectively. Starting from these raw data, we calculated peak velocity as the difference between maximal velocity reached in each condition and that reached in the corresponding baseline. Deceleration phase was computed as the difference between the percentage of deceleration phase observed in each condition's movement and that observed in the corresponding baseline. These two parameters are considered a hallmark of target uncertainty, with decreased peak velocity and increased deceleration phase indicating greater confound effect induced by the fake hand on the movement.

In humans, no significant result was found, neither for the velocity peak [main effect of *Position*: $F_{(1,19)} = .33$, $p = .57$; main effect of *Stimulation*: $F_{(1,19)} = 1.1$, $p = .31$; *Position by Stimulation* Interaction: $F_{(1,19)} = .1$, $p = .76$] nor for the deceleration phase [main effect of *Position*: $F_{(1,19)} = 1.05$, $p = .32$; main effect of *Stimulation*: $F_{(1,19)} = 1.84$, $p = .19$; *Position by Stimulation* Interaction: $F_{(1,19)} = 2.34$, $p = .14$]. In particular, the absence of a

Fig. 2 – **Results of the preliminary analyses comparing each kinematic parameter between internal and external baselines. Panel A, C and E represent the results of the analyses run on the human datasets regarding movement endpoint, velocity peak and deceleration phase respectively. Panel B, D and F represent the results of the analyses run on the monkey datasets regarding movement endpoint, velocity peak and deceleration phase respectively. Error bars represent standard error of the mean. Single subject values are displayed over each mean bar plot. Asterisks indicate significant results.**
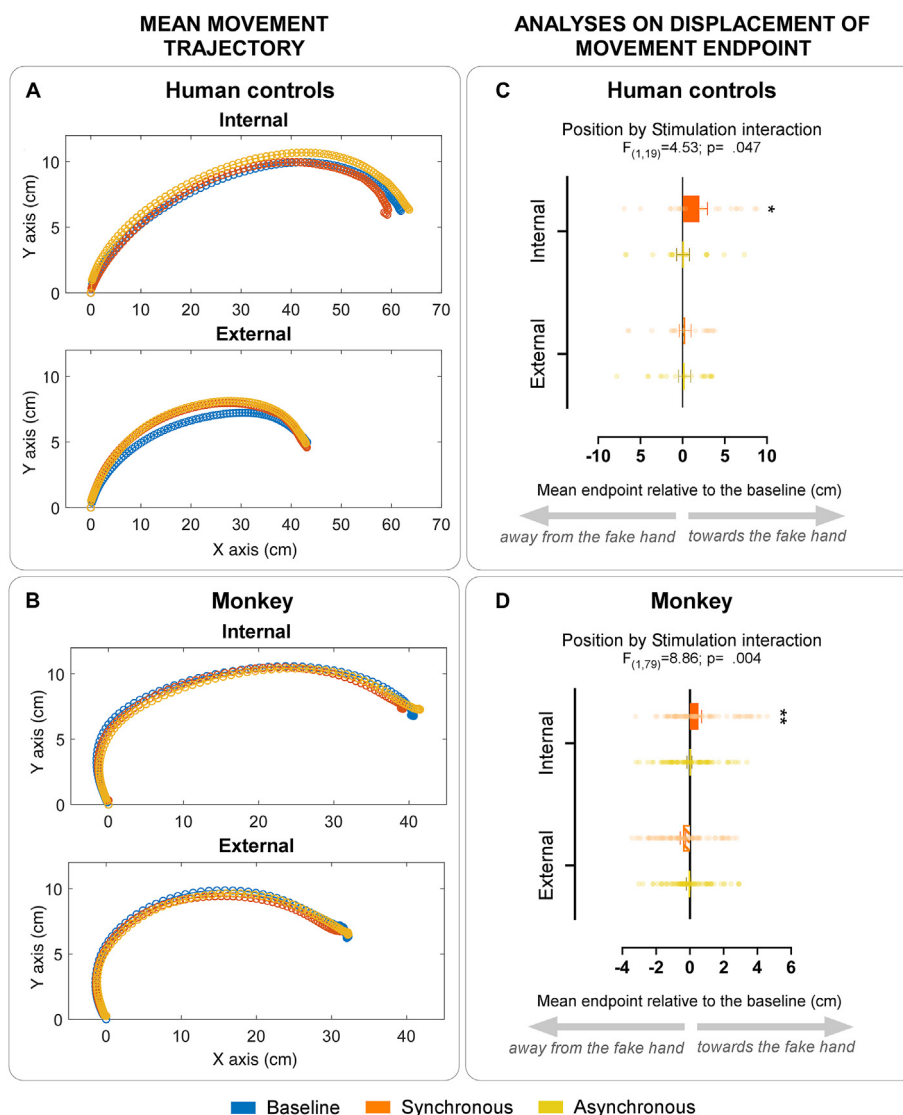
MEAN MOVEMENT TRAJECTORY

ANALYSES ON DISPLACEMENT OF MOVEMENT ENDPOINT

Fig. 3 − Left panels: mean trajectory of marker displacement (in x and y) for each of the four experimental conditions and the corresponding baselines, in both human controls (A) and monkey (B). Right panels: results of the analyses on mean displacement of movement endpoint regarding human controls (C) and the monkey (D). Error bars represent standard error of the mean. Single subject values for humans and single trial values for the monkey are displayed over the corresponding mean bar plot. Asterisks indicate significant results.

significant interaction seems to suggest that, differently from the displacement of movement's endpoint (see above), these two kinematic parameters are not sensitive to capture the modulation induced by the combination of bottom-up and top-down constraints in humans.

Mean velocity peak and mean deceleration phase in the monkey are shown in Fig. 5A and B, respectively. In the monkey, differently from humans, the velocity peak analysis shows a significant main effect of *Stimulation* [$F_{(1,79)} = 12.64$, $p = .0006$], with lower values in synchronous than asynchronous conditions, and *Position* [$F_{(1,79)} = 43.32$, $p < .0001$], with lower values in internal than external conditions (Fig. 5A). This means that both bottom-up and top-down constraints induce a decrease of the monkey's maximal velocity during the reaching movement, as if the animal was more uncertain.

Also the analysis of the deceleration phase seems to suggest a greater uncertainty of the monkey induced by the illusion (Fig. 5B). Here, the rmANOVA shows a significant main effect of *Stimulation* [$F_{(1,79)} = 4.89$, $p = .03$], with a longer deceleration phase in the synchronous than in the asynchronous condition and a significant *Position by Stimulation* interaction [$F_{(1,79)} = 10.95$, $p = .001$], suggesting that, when both bottom-up and top-down constraints make the attribution of the fake hand to the own body unlikely (i.e., in the asynchronous external condition), the deceleration phase is significantly lower with respect to the baseline, thus indicating smaller confound effect induced by the fake hand on the monkey's movement, as compared to all the other conditions (external asynchronous versus external synchronous: $p = .003$; external asynchronous versus internal
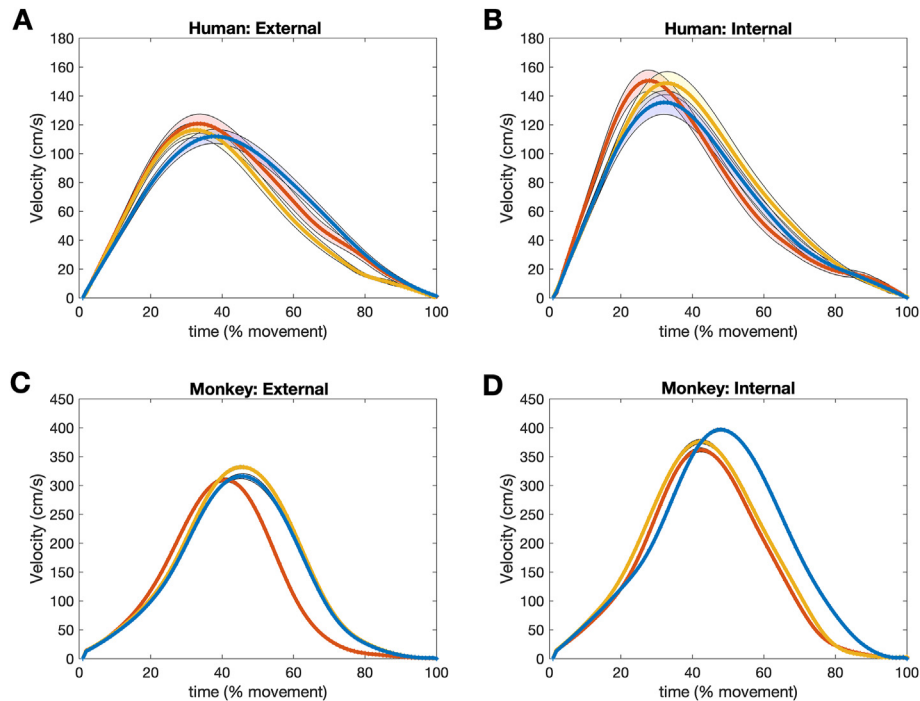
Fig. 4 — Mean velocity profiles of reaching movements performed by human controls (A–B) and monkey (C–D). Variability around the mean velocity indicates standard error of the mean.

asynchronous: $p = .006$; external asynchronous versus internal synchronous: $p = .035$) (Fig. 5B).

3.2. Explicit measures of RHI in humans

In human controls, to corroborate the results of the hand-identification reaching task with explicit reports of the illusory experience, we additionally collected subjective ratings at the Embodiment questionnaire (see Table 1). We computed an embodiment index (calculated as the difference between mean subjective ratings in real and control items), reflecting the subjective experience of embodiment of the fake hand.

As expected, the rmANOVA shows a significant *Position by Stimulation* interaction [$F_{(1,19)} = 5.53$; $p = .03$], with greater values in the Internal Synchronous condition as compared to all other conditions (internal synchronous versus internal asynchronous: $p = .001$; internal synchronous versus external synchronous: $p = .002$; internal synchronous versus external asynchronous: $p = .001$; Fig. 6). This result, in agreement with previous studies (Blanke et al., 2015), confirms that the embodiment of the fake hand is verified when both bottom-up and top-down constraints are respected (i.e., only in the internal synchronous condition). Crucially, these findings perfectly mirror the results found in the displacement of movement endpoint parameter, wherein the presence of a significant *Position by Stimulation* interaction revealed significantly greater attraction towards the fake hand position in the internal synchronous condition.

4.   Discussion

In the present study, we focused on the sense of body ownership (SBO) from an across-species perspective, by investigating whether similar bottom-up and top-down constraints that consent to build a SBO in humans also operate to build it in a Rhesus monkey. To this aim, the monkey and a cohort of human participants underwent a novel paradigm in which we combined the RHI procedure (Botvinick & Cohen, 1998) and a hand-identification reaching task borrowed from the clinical evaluation of patients with disorders of body-ownership (Errante et al., 2022; Garbarini et al., 2020; Pia et al., 2020; Rossi Sebastiano, Poles, et al., 2022). By measuring spatial and temporal kinematic features of self-directed movements during the illusion, this procedure allowed us to demonstrate that the embodiment phenomenon modulates the monkey's behavior according to human-like body ownership constraints.

Our results in human controls pinpoint that, by analyzing movement kinematics, we were able to capture the embodiment effect in individuals who also provided explicit report of illusory experience (i.e., subjective ratings at the Embodiment questionnaire). As expected, we replicated the classical RHI effect with significantly greater subjective ratings of embodiment of the fake hand following synchronous than asynchronous stimulation (Erro, Marotta, & Fiorio, 2020; Fossataro, Bruno, Giurgola, Bolognini, & Garbarini, 2018; Galigani,
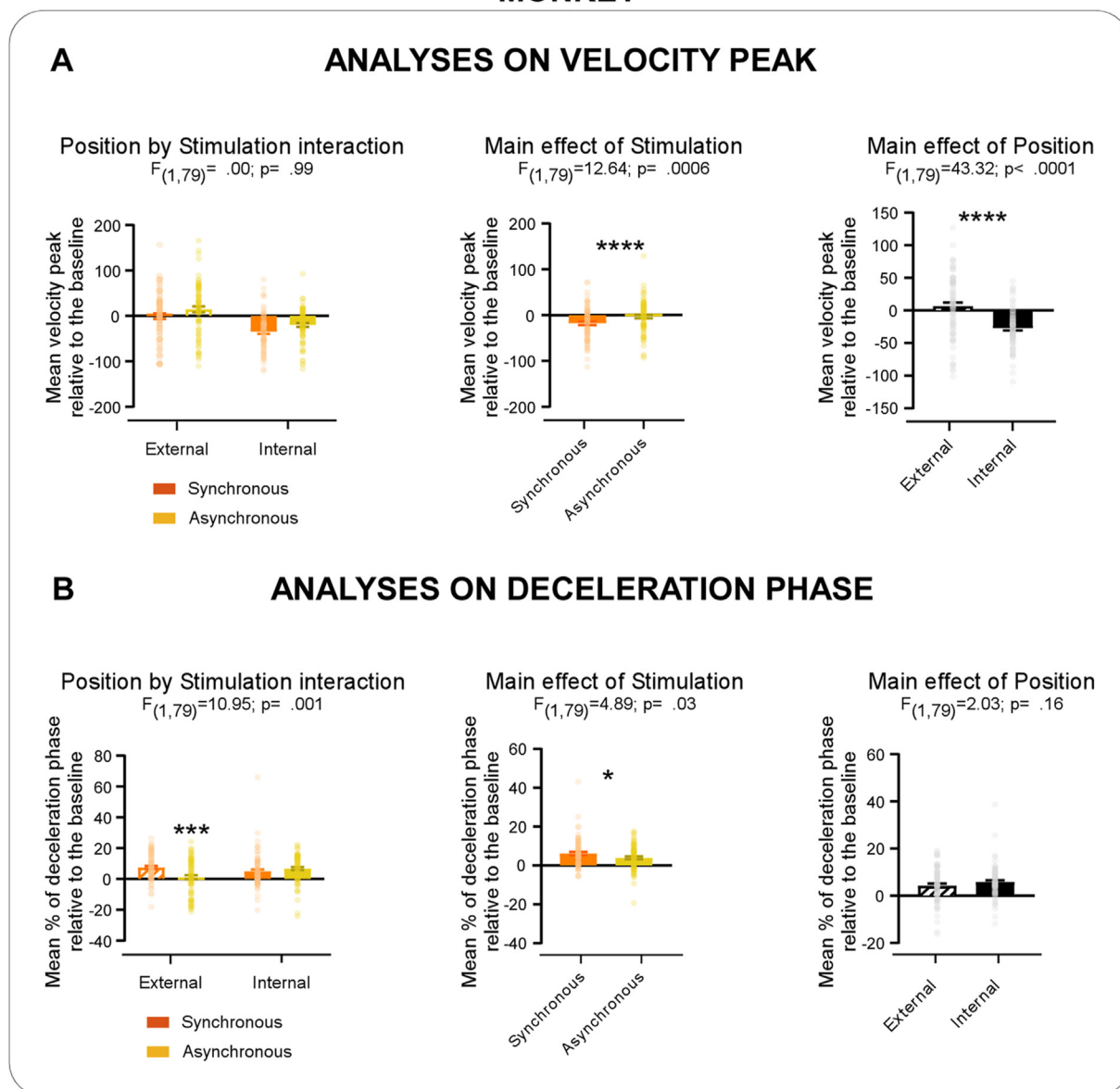
Fig. 5 — Panel A: Results of the analyses on velocity peak in the monkey. Panel B: results of the analyses on deceleration phase in the monkey. Error bars represent standard error of the mean. Single subject values are displayed over each mean bar plot. Asterisks indicate significant results.

Fossataro, Gindri, Conson, & Garbarini, 2022; Marotta, Zampini, Tinazzi, & Fiorio, 2018). Interestingly, this difference was modulated by the postural constraint, with significantly greater ratings of embodiment in the internal as compared to the external rubber hand position. Previous literature investigated the postural constraint by manipulating the perspective from which the fake hand was observed [i.e., first- *versus* third-person perspective; e.g., Bucchioni et al., 2016] or by manipulating its alignment with respect to the participant's shoulder (e.g., Erro et al., 2020). In line with such evidence, the synchronous internal condition was the one in which participants reported a greater illusion. Crucially, the very same modulation was observed also in the displacement of movement endpoint. Among the considered

kinematic parameters, this measure seems to be the one that captures embodiment more robustly. Indeed, when participants aimed to the own hand, the trajectory of self-directed movements was attracted by the position of the hand believed to be one's own (i.e., the fake hand). Similar kinematic parameters were previously employed by Kammers and colleagues (Kammers, de Vignemont, Verhagen, & Dijkerman, 2009) who, after inducing the illusion, asked participants to point on a board positioned over their deceived hand to indicate its felt position. The authors could not find a difference between RHI and control conditions, although, few years later, other research reported contrasting evidence, showing a shift in the pointed position following a different version of the RHI paradigm [i.e., visuo-motor RHI; (Kalckert & Henrik Ehrsson,
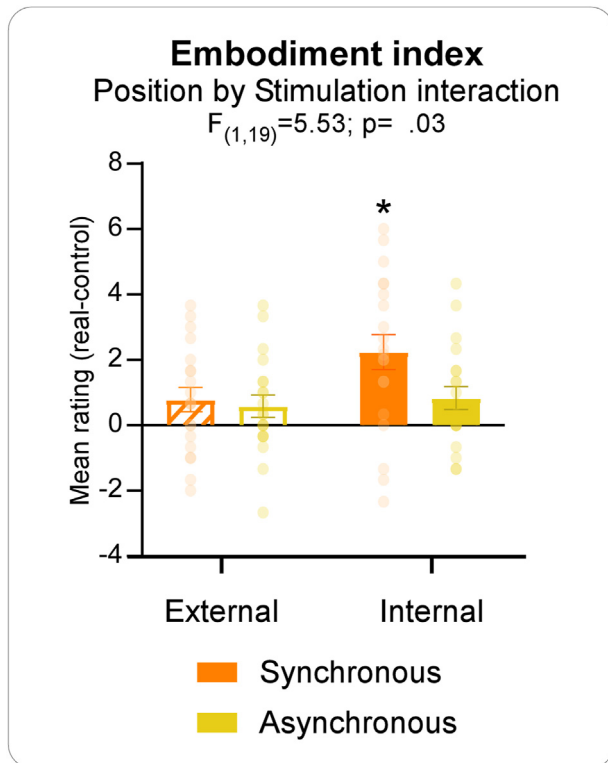
Fig. 6 − Results of the analyses on embodiment index (calculated as mean rating in real − control items of the Embodiment questionnaire) in human controls. Error bars represent the standard error of the mean. Single subject values are displayed over each mean bar plot. Asterisk indicates significant results.

2012)]. Irrespective of whether they found the effect or not, there are crucial differences between our procedure and those reported by previous studies that must be highlighted. In these studies, participants were asked to point at a board covering the hand subjected to the illusion, while the view of the rubber hand was precluded [as in classical proprioceptive drift procedures (Tsakiris & Haggard, 2005)]. By contrast, in our procedure, similarly to what happens during the motor evaluation of pathological embodiment (Errante et al., 2022; Garbarini et al., 2013, 2014, 2020; Pia et al., 2020; Rossi Sebastiano, Poles, et al., 2022), we asked participants to directly reach for their own hand while the view of the fake hand was allowed. This methodological aspect makes an important difference in terms of both kinematic recordings and maintenance of embodiment phenomenon. As regards kinematic recordings, movements which directly target the own body are characterized by specific kinematic patterns (Castiello & Dadda, 2019) which could be more sensitive to the body ownership manipulation. As regards the embodiment maintenance, viewing the rubber hand during reaching movements has likely maximized the embodiment maintenance during our hand-identification reaching task.

Crucially, the analysis on the displacement of movement endpoint shows an embodiment-dependent modulation not only in human controls but also in the monkey we tested here. Indeed, when both bottom-up and top-down constraints were

respected (i.e., only in the internal synchronous condition), the trajectory of the monkey's self-directed movements was significantly displaced towards the position of the fake hand. This finding, mirroring those of the human sample, suggests that also the monkey "*was fooled*" by the RHI in a similar way to human participants. Our results are in line with previous studies which employed the displacement of movement endpoint as an implicit marker to describe body ownership alterations both in patients with pathological embodiment (Rossi Sebastiano, Poles, et al., 2022), healthy participants undergoing the RHI (Rossi Sebastiano, Poles, et al., 2022; Zopf, Truong, Finkbeiner, Friedman, & Williams, 2011) and human (Bertoni et al., 2023) and non-human primates (Fang et al., 2019) subjected to a visuo-motor illusion. In particular, the preliminary results we show here in one monkey are in accordance with a previous study by Fang and collaborators (Fang et al., 2019) that measured modulations of the displacement of the movement trajectory following a visuo-motor illusion. However, it is worth noticing that these previous studies analyzed the motor parameters of the hand subjected to the illusion. By contrast, in our protocol, we analyzed the motor parameters of the non-deceived hand, similarly to the clinical evaluation of patients with pathological embodiment in which we capitalize on the motor parameters of the intact hand to identify the affected one. Our findings show that the monkey is deluded by the classical visuo-tactile RHI so that its motor system is biased toward the fake limb when aiming to the deceived hand with the non-deceived one. The behaviour of the monkey and human controls resembles the counterintuitive behaviour observed in brain-damaged patients with pathological embodiment. However, in the clinical context, the embodiment effect on the patients' motor behaviour is more dramatic, so that self-directed movements land right on top of the (embodied) alien hand, whenever it is placed in a body-congruent position (Garbarini et al., 2020). This greater magnitude of the embodiment effects in pathological as compared to experimental alterations of body ownership is in line with previous studies comparing these two contexts (Fossataro, Bruno, Gindri, et al., 2018; Rossi Sebastiano, Poles, et al., 2022).

Interestingly, in the monkey, besides displacement of movement trajectory, also other motor parameters showed sensitivity to the embodiment effect. Indeed, the embodiment modulates the monkey's motor behavior by decreasing the velocity peak and increasing the percentage of movement dedicated to deceleration. As regards velocity peak, it was reduced when, irrespective of the fake hand position, the visuo-tactile stimulation was synchronous or when, irrespective of the stimulation synchronicity, the position of the fake hand was body-congruent. In other words, when either bottom-up or top-down rules make the attribution of the fake hand to the own body more likely, then self-directed movements show an increased degree of uncertainty. This finding is in line with previous data in the human and monkey literature, showing that in goal-directed forelimb movements peak velocity is lower and deceleration phase is prolonged when the movement requires higher control (Castiello & Dadda, 2019; Fogassi et al., 1991, 2001; Roy et al., 2000, 2002). Complementary to the latter finding, the percentage of movement dedicated to deceleration was

decreased in the asynchronous external condition, when both bottom-up and top-down constraints were violated. In other words, when these two rules make the attribution of the fake hand to the own body more unlikely, then self-directed movements show an increased degree of certainty. This would indicate that, in the asynchronous external condition, the monkey relies more on the learned motor program, thus producing a ballistic movement, in which the proportion of deceleration phase typically decreases (Fogassi et al., 1991; Roy et al., 2000, 2002).

In conclusion, by borrowing the hand-identification reaching task from the pathological context, we were able to show in one individual monkey a behavioural counterpart of the neurophysiological evidence provided by Graziano's seminal studies (Graziano, 1999, 2000). In their pioneering works, these authors demonstrated that the monkey's neurons are modulated by the RHI, but whether the procedure was able to influence the monkey's behaviour remained unclear. Our results bring out preliminary evidence that *not only the monkey's neurons are fooled by the fake hand, but also the monkey's kinematic behaviour is*. If confirmed in a larger sample of monkeys, this finding should provide novel insights about both the plasticity of body ownership in monkeys and the constraints that regulate non-human body representations. By showing how these mechanisms are shaped within a phylogenetic perspective, the present study paves the way for future investigations adopting an ontogenetic perspective, to characterize their emergence through development.

Scientific transparency statement

DATA: All data supporting this research are publicly available: https://osf.io/uw4fb/
CODE: All analysis code supporting this research is publicly available: https://osf.io/uw4fb/
MATERIALS: All study materials supporting this research are publicly available: https://osf.io/uw4fb/
DESIGN: This article reports, for all studies, how the author(s) determined all sample sizes, all data exclusions, all data inclusion and exclusion criteria, and whether inclusion and exclusion criteria were established prior to data analysis.
PRE-REGISTRATION: No part of the study procedures was pre-registered in a time-stamped, institutional registry prior to the research being conducted. No part of the analysis plans was pre-registered in a time-stamped, institutional registry prior to the research being conducted.
For full details, see the Scientific Transparency Report in the online version of this article.

CRediT authorship contribution statement

A. Errante: Writing – review & editing, Writing – original draft, Visualization, Methodology, Investigation, Formal analysis, Data curation, Conceptualization. **A. Rossi Sebastiano:** Writing – review & editing, Writing – original draft, Visualization, Methodology, Investigation, Formal analysis, Data curation, Conceptualization. **N. Castellani:** Writing – review & editing, Methodology, Investigation, Formal analysis. **S. Rozzi:** Writing – review & editing, Methodology, Investigation, Conceptualization. **L. Fogassi:** Writing – review & editing, Supervision, Project administration, Funding acquisition, Conceptualization. **F. Garbarini:** Writing – review & editing, Supervision, Project administration, Funding acquisition, Conceptualization.

Funding

Open practices

The study in this article has earned Open Data badge for transparent practices. The data are available at: https://osf.io/uw4fb/.

Declaration of competing interest

The authors declare no competing financial of not financial interests.

Acknowledgments

Supplementary data

Supplementary data to this article can be found online at https://doi.org/10.1016/j.cortex.2024.10.011.

REFERENCES

Bertoni, T., Mastria, G., Akulenko, N., Perrin, H., Zbinden, B., Bassolino, M., et al. (2023). The self and the Bayesian brain: Testing probabilistic models of body ownership through a self-localization task. *Cortex; a Journal Devoted To the Study of the Nervous System and Behavior, 167*, 247–272. https://doi.org/10.1016/J.CORTEX.2023.06.019

Blanke, O., Slater, M., & Serino, A. (2015). Behavioral, neural, and computational principles of bodily self-consciousness. *Neuron, 88*(1), 145–166. https://doi.org/10.1016/j.neuron.2015.09.029

Botvinick, M., & Cohen, J. (1998). Rubber hands 'feel' touch that eyes see. *Nature, 391*(6669), 756. https://doi.org/10.1038/35784, 756.

Bruno, V., Sarasso, P., Fossataro, C., Ronga, I., Neppi-Modona, M., & Garbarini, F. (2022). The rubber hand illusion in microgravity and water immersion. *NPJ Microgravity, 8*(1), 15. https://doi.org/10.1038/s41526-022-00198-4. PMID: 35523786; PMCID: PMC9076892.

Bucchioni, G., Fossataro, C., Cavallo, A., Mouras, H., Neppi-Modona, M., & Garbarini, F. (2016). Empathy or ownership? Evidence from corticospinal excitability modulation during pain observation. *Journal of Cognitive Neuroscience, 28*(11), 1760—1771. https://doi.org/10.1162/JOCN_A_01003

Buckmaster, C. L., Rathmann-Bloch, J. E., de Lecea, L., Schatzberg, A. F., & Lyons, D. M. (2020). Multisensory modulation of body ownership in mice. *Neuroscience of consciousness, 2020*(1), Article niz019. https://doi.org/10.1093/nc/niz019

Castiello, U., & Dadda, M. (2019). A review and consideration on the kinematics of reach-to-grasp movements in macaque monkeys. *Journal of Neurophysiology, 121*(1), 188—204. https://doi.org/10.1152/JN.00598.2018

Castiello, U., Bennett, K. M. B., & Stelmach, G. E. (1993). The bilateral reach to grasp movement. *Behavioural Brain Research, 56*(1), 43—57. https://doi.org/10.1016/0166-4328(93)90021-H

Candini, M., Fossataro, C., Pia, L., Vezzadini, G., Gindri, P., Galigani, M., et al. (2022). Bodily self-recognition in patients with pathological embodiment. *Journal of Neuroscience Research, 100*(11), 1987—2003. https://doi.org/10.1002/JNR.25109

Castro, F., Lenggenhager, B., Zeller, D., Pellegrino, G., D'Alonzo, M., & Di Pino, G. (2023). From rubber hands to neuroprosthetics: Neural correlates of embodiment. *Neuroscience and Biobehavioral Reviews, 153.* https://doi.org/10.1016/J.NEUBIOREV.2023.105351

della Gatta, F., Garbarini, F., Puglisi, G., Leonetti, A., Berti, A., & Borroni, P. (2016). Decreased motor cortex excitability mirrors own hand disembodiment during the rubber hand illusion. *ELife, 5*(OCTOBER 2016). https://doi.org/10.7554/ELIFE.14972

Erro, R., Marotta, A., & Fiorio, M. (2020). Proprioceptive drift is affected by the intermanual distance rather than the distance from the body's midline in the rubber hand illusion. *Attention, Perception, and Psychophysics, 82*(8), 4084—4095. https://doi.org/10.3758/S13414-020-02119-7

Errante, A., Rossi Sebastiano, A., Ziccarelli, S., Bruno, V., Rozzi, S., Pia, L., et al. (2022). Structural connectivity associated with the sense of body ownership: A diffusion tensor imaging and disconnection study in patients with bodily awareness disorder. *Brain Communications, 4*(1), Article fcac032. https://doi.org/10.1093/BRAINCOMMS/FCAC032

Fogassi, L., Gallese, V., Gentilucci, M., Chieffi, S., & Rizzolatti, G. (1991). Kinematic study of reaching-grasping movements in the monkey. *Bollettino Della Società Italiana Di Biologia Sperimentale, 67*(7), 715—721. https://europepmc.org/article/med/1818597.

Fogassi, L., Gallese, V., Buccino, G., Craighero, L., Fadiga, L., & Rizzolatti, G. (2001). Cortical mechanism for the visual guidance of hand grasping movements in the monkey: A reversible inactivation study. *Brain: a Journal of Neurology, 124*(3), 571—586. https://doi.org/10.1093/BRAIN/124.3.571

Fossataro, C., Bruno, V., Gindri, P., Pia, L., Berti, A., & Garbarini, F. (2018). Feeling touch on the own hand restores the capacity to visually discriminate it from someone else' hand: Pathological embodiment receding in brain-damaged patients. *Cortex; a Journal Devoted To the Study of the Nervous System and Behavior, 104*, 207—219. https://doi.org/10.1016/j.cortex.2017.06.004

Fossataro, C., Bruno, V., Giurgola, S., Bolognini, N., & Garbarini, F. (2018). Losing my hand. Body ownership attenuation after virtual

lesion of the primary motor cortex. *The European Journal of Neuroscience, 48*(6), 2272—2287. https://doi.org/10.1111/EJN.14116

Fang, W., Li, J., Qi, G., Li, S., Sigman, M., & Wang, L. (2019). Statistical inference of body representation in the macaque brain. *Proceedings of the National Academy of Sciences of the United States of America, 116*(40), 20151—20157. https://doi.org/10.1073/PNAS.1902334116

Graziano, M. S. A. (1999). Where is my arm? The relative role of vision and proprioception in the neuronal representation of limb position. *Proceedings of the National Academy of Sciences of the United States of America, 96*(18), 10418—10421. https://doi.org/10.1073/pnas.96.18.10418

Gallagher, S. (2000). Philosophical conceptions of the self: Implications for cognitive science. *Trends in Cognitive Sciences, 4*(1), 14—21. https://doi.org/10.1016/S1364-6613(99)01417-5

Graziano, M. S. A., Cooke, D. F., & Taylor, C. S. R. (2000). Coding the location of the arm by sight. *Science, 290*(5497), 1782—1786. https://doi.org/10.1126/science.290.5497.1782

Garbarini, F., Pia, L., Piedimonte, A., Rabuffetti, M., Gindri, P., & Berti, A. (2013). Embodiment of an alien hand interferes with intact-hand movements. *Current Biology, 23*(2), R57—R58. https://doi.org/10.1016/j.cub.2012.12.003

Garbarini, F., Fornia, L., Fossataro, C., Pia, L., Gindri, P., & Berti, A. (2014). Embodiment of others' hands elicits arousal responses similar to one's own hands. *Current Biology, 24*(16), R738—R739. https://doi.org/10.1016/j.cub.2014.07.023

Garbarini, F., Fossataro, C., Pia, L., & Berti, A. (2020). What pathological embodiment/disembodiment tell us about body representations. *Neuropsychologia, 149*, Article 107666. https://doi.org/10.1016/J.NEUROPSYCHOLOGIA.2020.107666

Galigani, M., Fossataro, C., Gindri, P., Conson, M., & Garbarini, F. (2022). Monochannel preference in autism spectrum conditions revealed by a non-visual variant of rubber hand illusion. *Journal of Autism and Developmental Disorders, 52*(10), 4252—4260. https://doi.org/10.1007/S10803-021-05299-9

Jeannerod, M. (1984). The timing of natural prehension movements. *Journal of Motor Behavior, 16*(3), 235—254. https://doi.org/10.1080/00222895.1984.10735319

Jakobson, L. S., & Goodale, M. A. (1991). Factors affecting higher-order movement planning: A kinematic analysis of human prehension. *Experimental Brain Research, 86*(1), 199—208. https://doi.org/10.1007/BF00231054

Kalckert, A., & Henrik Ehrsson, H. (2012). Moving a rubber hand that feels like your own: A dissociation of ownership and agency. *Frontiers in Human Neuroscience, 6*, 19533. https://doi.org/10.3389/FNHUM.2012.00040

Kammers, M. P. M., de Vignemont, F., Verhagen, L., & Dijkerman, H. C. (2009). The rubber hand illusion in action. *Neuropsychologia, 47*(1), 204—211. https://doi.org/10.1016/J.NEUROPSYCHOLOGIA.2008.07.028

Longo, M. R., Schüür, F., Kammers, M. P. M., Tsakiris, M., & Haggard, P. (2008). What is embodiment? A psychometric approach. *Cognition, 107*(3), 978—998. https://doi.org/10.1016/J.COGNITION.2007.12.004

Messier, J., & Kalaska, J. F. (1999). Comparison of variability of initial kinematics and endpoints of reaching movements. *Experimental Brain Research, 125*(2), 139—152. https://doi.org/10.1007/S002210050669

Marotta, A., Zampini, M., Tinazzi, M., & Fiorio, M. (2018). Age-related changes in the sense of body ownership: New insights from the rubber hand illusion. *Plos One, 13*(11), Article e0207528. https://doi.org/10.1371/JOURNAL.PONE.0207528

Oldfield, R. C. (1971). The assessment and analysis of handedness: The Edinburgh inventory. *Neuropsychologia, 9*(1), 97—113. https://doi.org/10.1016/0028-3932(71)90067-4

Pia, L., Fossataro, C., Burin, D., Bruno, V., Spinazzola, L., Gindri, P., et al. (2020). The anatomo-clinical picture of the pathological

embodiment over someone else's body part after stroke. *Cortex; a Journal Devoted To the Study of the Nervous System and Behavior, 130*, 203—219. https://doi.org/10.1016/j.cortex.2020.05.002

Rossi Sebastiano, A., Bruno, V., Ronga, I., Fossataro, C., Galigani, M., Neppi-Modona, M., et al. (2022). Diametrical modulation of tactile and visual perceptual thresholds during the rubber hand illusion: A predictive coding account. *Psychological Research, 86*(6), 1830—1846. https://doi.org/10.1007/S00426-021-01608-0

Rossi Sebastiano, A., Poles, K., Miller, L. E., Fossataro, C., Milano, E., Gindri, P., et al. (2022). Reach planning with someone else's hand. *Cortex; a Journal Devoted To the Study of the Nervous System and Behavior, 153*, 207—219. https://doi.org/10.1016/J.CORTEX.2022.05.005

Roy, A. C., Paulignan, Y., Farnè, A., Jouffrais, C., & Boussaoud, D. (2000). Hand kinematics during reaching and grasping in the macaque monkey. *Behavioural Brain Research, 117*(1—2), 75—82. https://doi.org/10.1016/S0166-4328(00)00284-9

Roy, A. C., Paulignan, Y., Meunier, M., & Boussaoud, D. (2002). Prehension movements in the macaque monkey: Effects of object size and location. *Journal of Neurophysiology, 88*(3), 1491—1499. https://doi.org/10.1152/JN.2002.88.3.1491

Sartori, L., Camperio-Ciani, A., Bulgheroni, M., & Castiello, U. (2013). Reach-to-grasp movements in macaca fascicularis monkeys: The isochrony principle at work. *Frontiers in Psychology, 4*, 40209. https://doi.org/10.3389/FPSYG.2013.00114

Shokur, S., O'Doherty, J. E., Winans, J. A., Bleuler, H., Lebedev, M. A., & Nicolelis, M. A. L. (2013). Expanding the primate body schema in sensorimotor cortex by virtual touches of an avatar. *Proceedings of the National Academy of Sciences of the United States of America, 110*(37), 15121—15126. https://doi.org/10.1073/PNAS.1308459110

Tsakiris, M., & Haggard, P. (2005). The rubber hand illusion revisited: Visuotactile integration and self-attribution. *Journal of Experimental Psychology. Human Perception and Performance, 31*(1), 80—91. https://doi.org/10.1037/0096-1523.31.1.80

Wada, M., Takano, K., Ora, H., Ide, M., & Kansaku, K. (2016). The rubber tail illusion as evidence of body ownership in mice. *Journal of Neuroscience, 36*(43), 11133—11137. https://doi.org/10.1523/JNEUROSCI.3006-15.2016

Wada, M., Ide, M., Atsumi, T., Sano, Y., Shinoda, Y., Furuichi, T., et al. (2019). Rubber tail illusion is weakened in Ca2+-dependent activator protein for secretion 2 (Caps 2)-knockout mice. *Scientific reports, 9*(1), 7552. https://doi.org/10.1038/s41598-019-43996-9

Zopf, R., Truong, S., Finkbeiner, M., Friedman, J., & Williams, M. A. (2011). Viewing and feeling touch modulates hand position for reaching. *Neuropsychologia, 49*(5), 1287—1293. https://doi.org/10.1016/J.NEUROPSYCHOLOGIA.2011.02.012